Journal of Cleaner Production 394 (2023) 136356

Contents lists available at ScienceDirect

Journal of Cleaner Production

journal homepage: www.elsevier.com/locate/jclepro

Coagulation-flocculation of *Microcystis aeruginosa* by polymer-clay based composites

Ido Gardi [a], Yael-Golda Mishael [a], Marika Lindahl [b], Alicia M. Muro-Pastor [b], Tomás Undabeytia [c,*]

[a] The R.H. Smith Faculty of Agriculture, Food and Environment, The Hebrew University of Jerusalem, Rehovot, 76100, Israel
[b] Instituto de Bioquímica Vegetal y Fotosíntesis (IBVF), Consejo Superior de Investigaciones Científicas and Universidad de Sevilla, Centro de Investigaciones Científicas (CIC) Isla de la Cartuja. Avda, Américo Vespucio 49, 41092, Sevilla, Spain
[c] Instituto de Recursos Naturales y Agrobiología (IRNAS), CSIC, Reina Mercedes 10. Apdo. 1052, 41080, Sevilla, Spain

ARTICLE INFO

Handling Editor: Zhen Leng

Keywords:
Cyanobacteria
Polymer-clay composites
Surface waters
Coagulation-flocculation

ABSTRACT

Coagulation-flocculation is a critical treatment to reduce operational problems at Drinking Water Treatment Plants (DWTPs), created by episodes of cyanobacterial blooms in surface waters. There is a need for the search of good coaguflocculants that avoid release of intracellular toxins for a safer sustainable production. Clay-polymer interactions were examined for the development of efficient composites for their use as coaguflocculants for *Microcystis aeruginosa (M. aeruginosa)* suspensions. Polymers derived from poly-4-vinylpyridine (PVP) were quaternized on the pyridinic N by introducing methyl and hydroxyethyl moieties. These polymers were toxic *per se*; however, composites prepared either from their sorption or grafting on the clay surface of a montmorillonite exhibited null toxicity, The combination of infrared and X-ray diffraction data with thermal analysis showed a train conformation of the sorbed polymers on the clay surface whereas a brush conformation was elucidated for the grafted polymers. Only the composite prepared from grafting and subsequent quaternization with methyls was an efficient coagulocculant, due to its high positive surface potential (+39 mV) which allowed a close contact between the quaternary moieties of the brushes and the negative cell wall. A patch flocculation mechanism was involved, with the riks of resuspension of the coagulated cells if the composite added in excess. The optimum ratio between the amount of coagulated cyanobacteria and this composite expressed as equivalent to polymer content was 7.2×10^7 cells/mg polymer. This ratio was determined in axenic cultures of *M. aeruginosa*, but was reduced 5-fold in natural surface waters due to natural organic matter (NOM) content and heterogeneity. This study has demonstrated the relevance of the type of modification of the clay mineral surface with polymers to obtain good coagulocculants of cyanobacterial cells, that can be extended to other microorganisms.

1. Introduction

Cyanobacteria blooming episodes in water bodies are increasing due to global warming and nutrient enrichment arising from anthropogenic activities (Huisman et al., 2018). Their occurrence in water poses a risk for the environment and human health due to release of toxins. In addition, intracellular toxins can comprise more than 98% of the total amount (Du et al., 2017). Relevant cyanotoxins are cylindrospermopsin, anatoxin-a, saxitoxins and microcystins (MCs) (Du et al., 2019). MCs are of special concern due to their ubiquity, high hepatotoxicity and resistance to degradation because of their cyclic peptide structure (He et al., 2016). Numerous intoxication events by MCs have been reported not only due to recreational exposures for humans and domestic animals but also linked to potable surface waters causing outbreak diseases (Backer et al., 2015). Although there are more than 100 congeners of MCs, only four of them are of special significance because of their toxicity (LR, RR, LA and YR) (Westrick et al., 2010). The WHO has established a guideline value of 1 μg L^{-1} for MC-LR in drinking waters.

Moreover, the occurrence of cyanobacteria can create operational problems in DWTPs such as clogging of filters, inefficient disinfection, increased organic loading into water, reduced lifespan of membranes, generation of disinfection by-products, penetration of cells into the final treated water and distribution system, etc. (Sorlini et al., 2018). Coagulation-flocculation has been proved to be a key treatment for removal of cyanobacterial cells along DWTPs avoiding the release of

* Corresponding author.
E-mail address: undabeyt@irnase.csic.es (T. Undabeytia).

https://doi.org/10.1016/j.jclepro.2023.136356
Received 10 September 2022; Received in revised form 25 January 2023; Accepted 3 February 2023
Available online 7 February 2023

Abbreviations used:

M. aeruginosa	*Microcystis aeruginosa*
MC	microcystin
QPVP	quaternized polyvinylpyridine
MMT	montmorillonite
PGC	grafted PVP composite
APTES	aminopropyltriethoxysilane
DMF	N,N-dimethylformamide;
BIB	2-bromoisobutyryl-bromide
NaPPi	tetrasodium pyrophosphate
QPVP	PGC quaternized with methyls
OH-QPVP	PGC quaternized with hydroxyethyl moieties
FMC	flow citometry
FTIR	Fourier transform infrared
XRD	X-ray diffraction
DSC	differential scanning calorimetry
Tg	glass transition temperature
ROS	reactive oxygen species
H_2DCFA	2′-7′-dichlorofluorescein diacetate
DIBAC4(3)	Bis(1,3-dibutylbarbituric acid) trimethine oxonol
NOM	natural organic matter

endotoxins by cell lysis (Ghernaout et al., 2010). Cationic coagulants are very effective due to the fact that cyanobacteria cells are negatively charged at natural pH (6.5–8.5) due to dissociation of functional groups, mainly carboxylic, at the cell surface (Henderson et al., 2008). Metal coagulants based on Al and Fe in the form of salts such as aluminium sulphate, ferric chloride, ferric sulphate; or as inorganic polymers (polyferric sulphate, polyaluminium chloride) are widely used (Lal and Garg, 2019). The hydrolysis of the metals yields positively charged hydroxides that neutralize or reduce the charge of the cell surface leading to destabilization. The use of cationic organic polyelectrolytes instead permits the application of lower doses (Tran et al., 2013), minimizing the risks associated with residual Al intake from tap water or deterioration of the distribution system by formation of corrosive products when Fe coexists with chloride anions (Huh and Ahn, 2017). In these cases, destabilization of the cyanobacterial suspensions is mainly carried out by an interparticle bridging mechanism. The negatively charged surface sites of different cells are neutralized by cationic segments of the polymer molecule (Theng, 2012). Polymers such as cationic polyacrylamides (König et al., 2014) and starch (Letelier-Gordo et al., 2014) are very efficient coagulants, whereas chitosan is only efficient at pH below 8.0 due to loss of its positive charge (Gerchman et al., 2017). The most important features of the polymers that determine their performance in coagulation-flocculation processes are their molecular weight and charge density, but in general, the yields are very low in the case of waters of very low turbidity and the use of aids such as clay minerals is necessary (Ghernaout and Ghernaout, 2012). In this context, the combined use of cationic polymer and clay minerals can be a good alternative for their use in coagulation-flocculation of cyanobacterial suspensions. In the design of a polymer-clay mineral complex acting as a coagulflocculant, a parameter to be controlled is that polymer desorption is negligible, since the presence of polymer molecules could cause operational problems in subsequent water treatment units such as membrane fouling in nano and ultrafiltration processes, pasivation of granular activated carbon or the formation of disinfection by-products. In general, adsorption of polycations on clay minerals is considered to be irreversible due to the numerous contact points between the clay surface and the cationic segments. However, experimental evidence indicates that a certain fraction can be desorbed (Ganigar et al., 2010). This fraction is related to the conformation of the polymer on the clay surface. A train-shaped conformation is desirable in coagulation-sedimentation studies because in a loop-and-tails conformation, a fraction of the adsorbed polymer is loosely associated with the clay resulting in it is desorption (Kohay et al., 2015). Another approach to avoid polymer desorption consists in the production of composites in which the polycation is grafted on the surface of the clay (Gardi and Mishael, 2018). Both types of composites will be examined in this study to determine and compare their effectiveness as coagulflocculants of cyanobacterial suspensions.

The polymers used were quaternized polyvinylpyridine, which were sorbed and grafted on the surface of the clay mineral montmorillonite. Quaternization was performed by introducing methyl and hydroxyethyl moieties on the pyridinic N. Although the presence of quaternary ammoniums in organic substances poses a biocidal character, this study determined the conditions for obtaining composites made of these polycations with clay minerals as good coagulflocculants that prevent cell rupture and the release of endotoxins. The objectives of the current work were: (i) to design clay-polycation complexes with negligible desorption of the polymer, by using sorption and grafting processes; (ii) to test their efficiency as coagulflocculant of *M. aeruginosa* suspensions; and (iii) to study the flocculation mechanisms involved.

2. Materials and methods

2.1. Materials

Montmorillonite clay, SWy-2 (MMT) was purchased from Source Clay Repository (Clay Minerals Society, Columbia, MO, USA). PVP, 4-vinylpyridine (4-VP), 3-aminopropyltriethoxysilane (APTES), 2-bromoisobutyryl-bromide (BIB), glycerol, anhydrous toluene and trimethylamine (TMA), 2-bromo-ethanol, 2-iodomethanol, N,N-dimethylformamide (DMF), ethanol, formic acid (FA), H_2SO_4, HCl, $CuCl{\cdot}H_2O$ and $CuCl_2$ were provided by Merck Co. (Darmstadt, Germany). MC-LR was purchased from Enzo Life Sciences Inc. (Farmingdale, NY, USA). The fluorescent probes 2′,7′-dichlorofluorescein diacetate (H_2DCFDA) and bis(1,3-dibutylbarbituric acid) trimethine oxonol (DIBAC4(3) were supplied by Invitrogen Molecular Probes (Eugene, OR, USA). High Performance Liquid Chromatography (HPLC)-grade acetonitrile and water were obtained from Teknokroma S.A. (Barcelona, Spain).

Microcystis aeruginosa PCC7806 (hereafter referred to as *Microcystis* sp.) was obtained from the CIC Isla de la Cartuja Biological Cultures Service. Cyanobacteria bloom surface water was collected from a water reservoir located in Carrión de los Céspedes (Sevilla, Spain).

2.2. Methods

2.2.1. Preparation of grafted PVP composite

The stages in montmorillonite surface modification include a series of succesive stages as described in Gardi and Mishael (2018) followed by quaternization of the grafted composite: 1. *Acid activation and amination of montmorillonite surface*. Briefly, sulfuric acid was added to a 5% MMT suspension under stirring and the total acid concentration was 1%. After stirring for 120 min, the solid was then washed with distilled water and freeze-dried. Thereafter, the dry aa-MMT (10 g) was suspended in a 500 mL mixture of ethanol and water (3:1) under reflux at 80 °C. APTES (6.24 mL) was added dropwise and the temperature was raised to 95 °C for 24 h. The solids were separated by centrifugation, washed thoroughly with ethanol and water and freeze dried. 2. *Initiation of aminated montmorillonite*: Dry acid activated APTES grafted montmorillonite (aa-MMT-ATPES) (5 g) was suspended in 40 mL anhydrous toluene and 10 mL anhydrous trimethylamine. The suspension was cooled down to 0 °C in an ice bath. BIB (5 mL) mixed in 30 mL anhydrous toluene was added dropwise to the cold suspension. Then the ice bath was removed, and the reaction was carried out at ambient temperature for 24 h. aa-MMT-ATPES-BIB was then separated by centrifugation, thoroughly washed with toluene and acetone, dried at 105 °C overnight and kept in

a desiccator. 3. *Surface initiated – atom transfer radical polymerization (SI-ATRP) of PVP from initiated montmorillonite*: aa-MMT-ATPES-BIB (1.1 g) was suspended in a 140 mL 1:1 glycerol water mixture. $CuCl{\cdot}H_2O$ (20.4 mg), $CuCl_2$ (59.4 mg) and Tris(2-dimethylaminoethyl) amine (384 μL) were added to the suspension. The suspension was degassed by 3 cycles of freeze-pump-thawing and the frozen suspension was allowed to thaw under a N_2 stream. VP monomers (3.2 mL) were mixed in a 100 mL glycerol water mixture (which also underwent freeze-pump-thawing), the monomer solution was slowly added dropwise to the initiated clay suspension. The polymerization reaction was carried out at 90 °C under N_2 atmosphere for 24 h. The polymerization reaction was terminated by adding dropwise a 1:9 HCl and methanol mixture (5 mL). The grafted PVP-clay composite (PGC) was thoroughly washed with ethanol and an ethanol/water mixture containing 1% HCl, freeze-dried and stored in a desiccator. 4.*Monomer quaternization.* It was performed by interacting PGC with 2-bromo-ethanol or 2-iodomethanol producing OH-PGC or CH_3-PGC. OH-PGC was prepared by suspending 1 g of dry PGC in 70 mL anhydrous ethanol. The suspension was heated to 80 °C under reflux. Then 1 mL of 2-bromoethanol in 100 mL ethanol was added dropwise to the suspension which was left overnight. The modified composite was dried in a rotary evaporator, washed with distilled water and freeze-dried. CH_3-PGC was prepared by suspending 1 g of PGC in 70 mL DMF at 60 °C under reflux, then 1 mL of 2-iodomethanol in 100 mL DMF was added dropwise to the suspension and left overnight. The suspension was then centrifuged and the precipiate was washed with ethanol and water and finally freeze-dried.

2.2.2. Preparation of quaternaries poly vinylpyridine

Quaternization of PVP was preformed by reacting the polymer with 2-bromo-ethanol or 2-iodomethanol producing OHQPVP or QPVP, respectively. In order to prepare OH-QPVP, 3 g PVP was dissolved in 100 mL ethanol at 80 °C and 3 mL 2-bromo-ethanol in 100 mL ethanol was then added dropwise to the polymer. After 2 h, the polymer was dried in rotary evaporator. In order to prepare QPVP, 3 g of PVP was dissolved in 100 mL DMF at 60 °C and 3 mL 2-iodomethanol in 100 mL ethanol was then added dropwise to the polymer. After 24 h, the polymer was dried in rotary evaporator.

2.2.3. Preparation of adsorbed composites

In order to adsorb the quaternized polymers, OHQPVP and QPVP to MMT, polymer solutions of 3 g L^{-1} were added to MMT yielding a clay suspension of 5%. After shaking for 24 h, the suspensions were centrifuged and lyophylized yielding the composites denoted by OH-MMT and CH_3-MMT from sorption of the polymers OHQPVP and QPVP, respectively.

2.2.4. Characterization of polymers and composites

Characterization was performed as follows: Fourier transform infrared (FTIR) spectra were recorded using a Nicolet 6700 (Thermo Waltham, MA, USA) FTIR spectrometer equipped with an attenuated total reflection module. The surface zeta potential was measured using a Zetasizer Nano ZS (Malvern, UK). Elemental analysis of C and N was performed with a CHNSO elemental analyzer TRUSPEC CHNS MICRO (Leco Co., MI, USA). X-ray diffraction (XRD) of oriented samples were recorded with an X-ray diffractometer D8 Advance A 25 (Bruker, MA, USA). Differential scanning calorimetry (DSC) measurements were performed using a DSC-Q20 (TA Instruments, DE, USA). Measurements were recorded at heating from 0 °C to 260 °C and succesive cooling rate of 10 °C/min under a nitrogen atmosphere at 100 mL/min flow. Tg was determined in the second heating process.

2.2.5. Toxicity assays

Microcystis sp. was grown in BG11 medium supplemented with 17.5 mM $NaNO_3$ and 10 mM $NaHCO_3$, under a bubbling mixture of CO_2 in air (1% v/v) at 30 °C, and with a light intensity of 75 μE m^2 s^{-1} under continuous light. The concentration of this suspension was determined by flow cytometry (FCM), from which the suspensions subsequently used were prepared by dilution with distilled water, and their concentrations were also checked by cytometry. In the toxicity studies, a cell suspension of 3.71×10^6 cells/mL was incubated with polymer solutions, their final concentrations ranging from 5 to 50 mg/L. After shaking at 700 rpm for 1 or 24 h, the suspensions were analyzed by flow cytometry.

2.2.6. Flow cytometric analysis

A FC500 flow cytometer (Beckman Coulter, USA) equipped with an air cooled 20 mW argon laser and an additional red diode laser emitting at the fixed wavelengths of 488 and 630 nm, respectively, was used for measurement. Fluorescent filters and detectors were all standard with green fluorescence collected in channel FL1 (525 nm) and red fluorescence in channel FL4 (675 nm). Probe fluorescence, chlorophyll *a* fluorescence, forward scatter-FSC (cell size) and side scatter-SCC (cell granularity) data were collected and analyzed using CXP software. FSC, FL4 were used to quantify and gate the cyanobacterial cells based on their chorophyll red autofluorescence. The histogram plot was divided into two regions: counting of particles emitting fluorescence assigned to live cells, and particles with no emission of fluorescence assigned to dead cells. FSC was previously fitted to determine only cyanobacteria.

The generation of ROS in cyanobacterial suspensions in the presence of polymer solutions (0–50 mg/L) was assessed by loading the cells with the fluorescent dye H_2DCFDA. This compound is converted by cellular esterases into the non-fluorescent compound 2,2-dichlorodihydrofluorescein (H_2DCF), that after oxidation is transformed into the fluorescent 2,7-dichlorofluorescein (DCF), serving as an indicator for hydrogen peroxide and other ROS (Gomes et al., 2005). A 10 mM H_2DCFDA stock solution was freshly prepared in DMSO under dim light conditions. One mL of the culture was centrifuged, resuspended in BG11 medium containing H_2DCFDA and polymer solutions, and incubated for 1 h in darkness. The final concentration of H_2DCFDA was 1 μM, and the polymer solutions were 20 mg/L. After 30 min of incubation in ambient light, the suspensions were analyzed by flow cytometry. As a positive control, addition of methyl viologen (100 μM) was used.

As an indicator of the changes in membrane potential of the cells, the DIBAC4(3) probe was used. Again, one mL of the culture was centrifuged, and resuspended in BG11 medium containing 5 μL of 1 μg/mL of the fluorescent probe, and polymer solutions at a final concentration of 20 mg/L. After incubation for 20 min in darkness at room temperature, the suspensions were analyzed.

The analyses of DIBAC4(3) and DCF were performed by collecting their green fluorescence with the 530/30 nm band pass filter (FL1).

2.2.7. Coagulflocculation tests

100 mL of an axenic cyanobacterial culture (3.71×10^6 cells/mL) was placed into 250 mL beakers. A magnetic stirrer was inserted and the different amounts of composites containing each one 20 mg/L of the polymer, were added at 700 rpm. After 1 h, the stirring was slowed down to 200 rpm for 15 min. After settling times of 15 min, the cyanobacterial concentration, the zeta potential and the turbidity in the upper part of the supernatants, were measured. Residual turbidity was calculated as the fraction remaining in the supernatant from the initial value (expressed as percent). This experimental procedure was also performed for an initial period of 24 h stirring. The influence of experimental conditions as the rapid mixing time (5–60 min), temperature (25-40 °C) and initial pH (4.4–7.7, adjusted by using aliquots of HCl and NaOH) were studied.

In another experiment, coagulflocculation tests were performed with the CH_3-PGC composite at amounts equivalent to polymer concentrations ranging from 1 to 40 mg/L. A parallel experiment was performed but using surface waters instead (Table S1). Their SUV_{254} values were determined based on the analysis of the organic carbon after filtration of water samples through 0.22 μm membrane filters (Prat Dumas, France) by using a Shimadzu TOC-VSCH analyzer and an UV–Visible Shimadzu

model 1201 spectrophotometer.

The coagulated cells with the polymer CH_3-PGC were extracted by dilution with a 0.01 M tetrasodium pyrophosphate (PPiNa) solution. After shaking for 30 min at 300 rpm, the samples were sonicated inside ice three times at 40 s (80 W, frequency 25 cycles) followed by centrifugation at 1000*g* for 1 min. An aliquot (5 μL) was mixed with 1X TE (495 μL) and analyzed by FCM.

2.2.8. Microcystin analysis

The analysis of MC-LR was performed on a HPLC (Agilent 1290) connected to a triple-quadrupole mass spectrometer (ABSCIEX 3200 QTRAP; Agilent Technol., CA, USA) with an electron ion spray source working in positive mode. The flow rate was 0.3 μL/min, the column was an Eclipse XDB-C18 (150 × 3.0 mm I.D.; 3.5 μm) operating at 40 °C and the injection volume was 20 μL. The binary mobile phase in gradient mode consisted of ultrapure water (UPW) (mobile phase A) and ACN (mobile phase B), both with a content of 0.1% FA. The gradient used was from 0 to 2.0 min, isocratic (95% A: 5%B); from 2.0 to 7.0 min, a linear increase of B from 5% to 40%; from 7.0 to 9.0, B increased from to 40–50%, another increase in B from 9 to 17 min up 70% that was maintained isocratically for 1 min; and finally a lineal decrease of B to 5% from 18.0 to 20.0 min. Quantification was made by using the transition for Q1 995.58-Q3 135.30 m/z. The limit of detection (LOD) was 0.1 μg L^{-1} and the retention time was 10.49 min.

2.2.9. Confocal laser scanning microscopy

Confocal laser scanning microscopy (CLSM) was performed with a Leica SP2 using a HCX PL APO 63 × 1.4 NA oil immersion objective. Coaguflocculated sample of cyanobacteria with CH_3-PGC after 1 h incubation was analyzed. The sample was excited with 488 nm laser and fluorescence emission was detected between 500 and 540 nm for supporting composite and between 650 and 700 for cell auotofluorescence (Chlorophyll). Differential Interference Contrast (DIC) images were monitored on transmitted light channel.

3. Results and discussion

3.1. Characterization of the clay-polymer composites

3.1.1. Polymer loading

The polymer loading in the composites prepared by sorption was 4.3 and 6.9% w:w for the OHQPVP- and QPVP-based composites, respectively. In contrast to these low values, the amount of grafted polymer increased to 33% and 29% for the OHQPVP- and QPVP-based composites, respectively. In spite of the higher content of polymers on the grafted composites, the surface charge only increased slightly when the polymer was grafted relative to the sorbed (Fig. 1a).

3.1.2. Infrared spectroscopy

The infrared spectra showed typical absorption bands due to ring stretching of pyridinium ions at 1645, 1573 and 1516 cm^{-1} for both polymers (Fig. 1b). However, the presence of a band around 1600 cm^{-1} that is typical of pyridyl rings ($V_{C=N}$ vibration) denoted incomplete quaternization of the OHQPVP polymer. The fraction of quaternized monomers can be roughly calculated from the band intensities at 1645 and 1606 cm^{-1} using the ratios between these two bands from the study of Levy et al. (2019), who quaternized a related polymer (PVP-coSt) at several ratios. The fraction of quaternized monomers in the OHQPVP polymer was estimated to be 82% of the total. In contrast, the QPVP polymer was fully quaternized as no absorption was noted at 1606 cm^{-1}. The absorption band at 1471 cm^{-1} was due to CH_2 scissoring. After sorption of both polymers on the clay, a new absorption band appeared at a higher wavelength, 1662 cm^{-1}, indicating an increase in ring stiffness, which is due to electrostatic interactions between pyridinium monomers with the cationic exchange sites of the clay.

Grafting of the polymers on the clay followed by further quaternization showed the same pattern as with the polymers. The OHQPVP grafted was not fully quaternized, as evidenced by the presence of the pyridyl ring absorption band at 1606 cm^{-1}, whereas quaternization was complete in the QPVP grafted.

3.1.3. Thermal analysis

The DSC curve of both polymers revealed glass transition temperatures (Tg) at 124 and 180 °C for OHQPVP and QPVP polymers, respectively (Fig. S1). These Tg were no longer present in the sorbed and grafted polymers (Fig. S2), that is explained by restricted movement of the polymer segments. After sorption, the electrostatic interactions between the positively charged monomers and the clay platelets lead to restricted motion of the polymer. The conformation of the polymers on the clay surface will be a function of their loading and the concentration of positively charged monomers, which in turn depends on the degree of quaternization of the pyridinyl N. As the charge density of the polymer increases, its conformation shifts from a "loops and tail" conformation to one more extended ("trains") (Kohay et al., 2019). In addition, a low

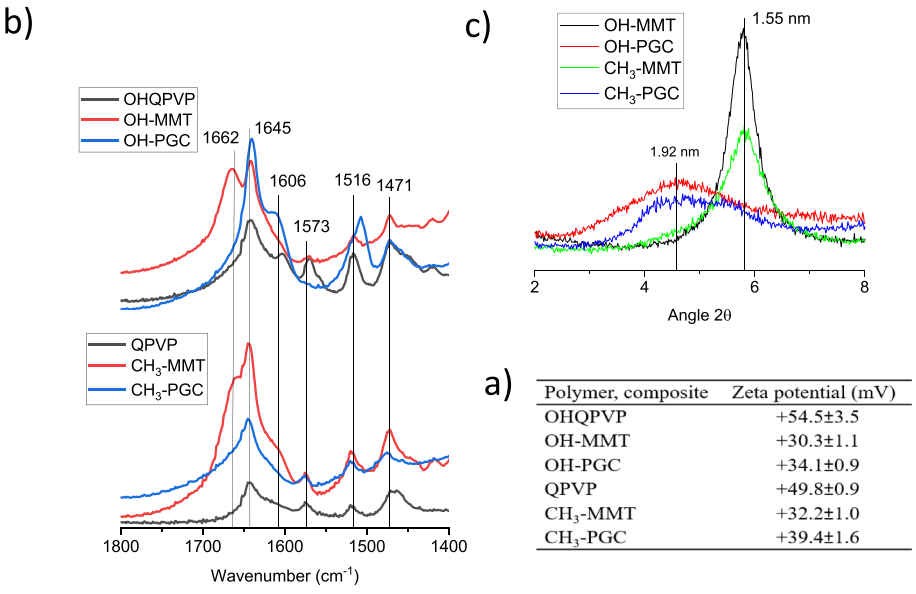

a)

Polymer, composite	Zeta potential (mV)
OHQPVP	+54.5±3.5
OH-MMT	+30.3±1.1
OH-PGC	+34.1±0.9
QPVP	+49.8±0.9
CH_3-MMT	+32.2±1.0
CH_3-PGC	+39.4±1.6

Fig. 1. Characterization of polymer and clay-polymer clay composites: (a) zeta potential values; (b) FTIR spectra; and (c) X-ray diffractograms.

loading of the polymer was reported to adopt a train conformation by using a fully quaternized polymer, whereas at high loading, the composite presented a microstructure with layers of polymers between the clay platelets and polymer molecules on the external surface with a configuration of loops and tails (Kohay et al., 2015). These molecules on the external surface were easily detached unlike those intercalated, the desorption of which was negligible. The low loading of the polymers on these composites suggested a train configuration of the polymer.

3.1.4. X-ray diffraction

A train conformation with the composites obtained by sorption was corroborated by XRD that showed a basal spacing of 1.55 nm (Fig. 1c). This d-spacing has been in general ascribed to this conformation (Undabeytia et al., 2014), and by the dissapearance of Tg in both composites, which would have been detected in the presence of loosely associated molecules.

In the grafted polymers, the polymer chains can adopt a stretched conformation or a more relaxed conformation in the vicinity of the clay surface, that will be determined by the grafting density and the degree of polymerization (Zhuo et al., 2017). If the grafting density is high, the excluded volume interactions yield more stretched chain conformations, the so-called "brush" conformation (Dang et al., 2013). The high amounts of polymer tethered on the surface of these composites, together with the absence of Tg due to confinement of polymer chains limiting their movement, pointed towards a brush conformation. X-ray difraction of the grafted composites showed a very broad and non-symmetric peak at about 1.92 nm (Fig. 1c). This pattern may be indicative of polymer inhomogeneity during the course of polymerization.

3.2. Effect of polymer concentration on cyanobacteria survival

Cyanobacterial survival was strongly dependent on the polymer used as well as its concentration. Whereas the polymer QPVP hardly affected the status of *M. aeruginosa* in solution, even at high concentrations, the OHQPVP polymer induced cell death within 1 h at concentrations as low as 5 mg/L, with a survival rate of about 65% (Fig. 2). After 24 h incubation, cell survival was almost null with the polymer OHQPVP. In constrast, only at high concentrations of QPVP, the survival rate was close to that observed with OHQPVP. A 5 mg/L concentration of OHQPVP induced the same toxicity as a 10-fold higher concentration of QPVP, revealing a more toxic character of the polymer when a hydroxyl moiety is introduced.

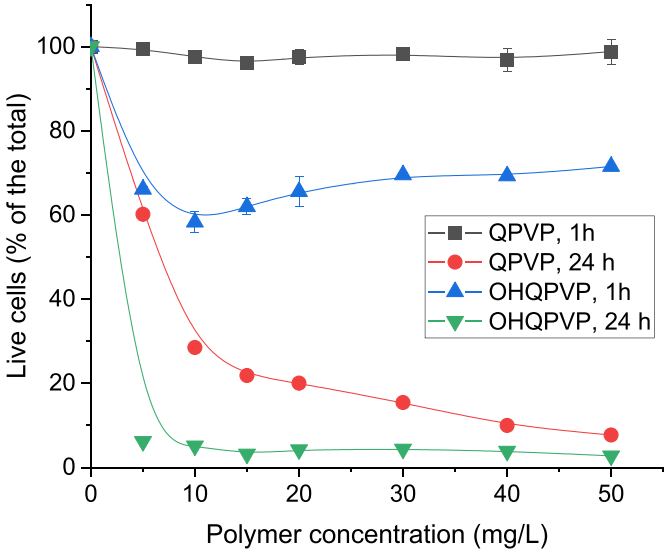

Fig. 2. Effect of polymer concentration on cyanobacterial survival. The *M. aeruginosa* concentration was 3.71 × 10^6 cells/mL.

In order to elucidate the mechanisms involved in the toxicity of QPVP and OHQPVP, their effects on the photosynthetic machinery and barrier permeability were examined through the use of the fluorescent probes H_2DCFA and DIBAC4(3), respectively (Fig. 3). The experimental conditions were modified by using a higher polymer/cell concentration ratio. In this way, the effect produced by the QPVP polycation can be also visualized.

In Fig. 3a, both polymers induced a decrease in the fluorescence of DIBAC4(3) as reflected in the downward shift of the control-related peak. The fluorescence intensity values were normalized to the live cell content, thus eliminating any variation in these values due to the killing effect of the polymers. These downward shifts are associated with a more negative transmembrane potential (hyperpolarization). DIBAC4(3) *per se* has a very low fluorescence in the external medium, but when it is bound to the hydrophobic core of the lipid membrane its fluorescence increases (Wolff et al., 2003). Therefore, as the inside of the cyanobacterial cell became more negatively charged, leading to a

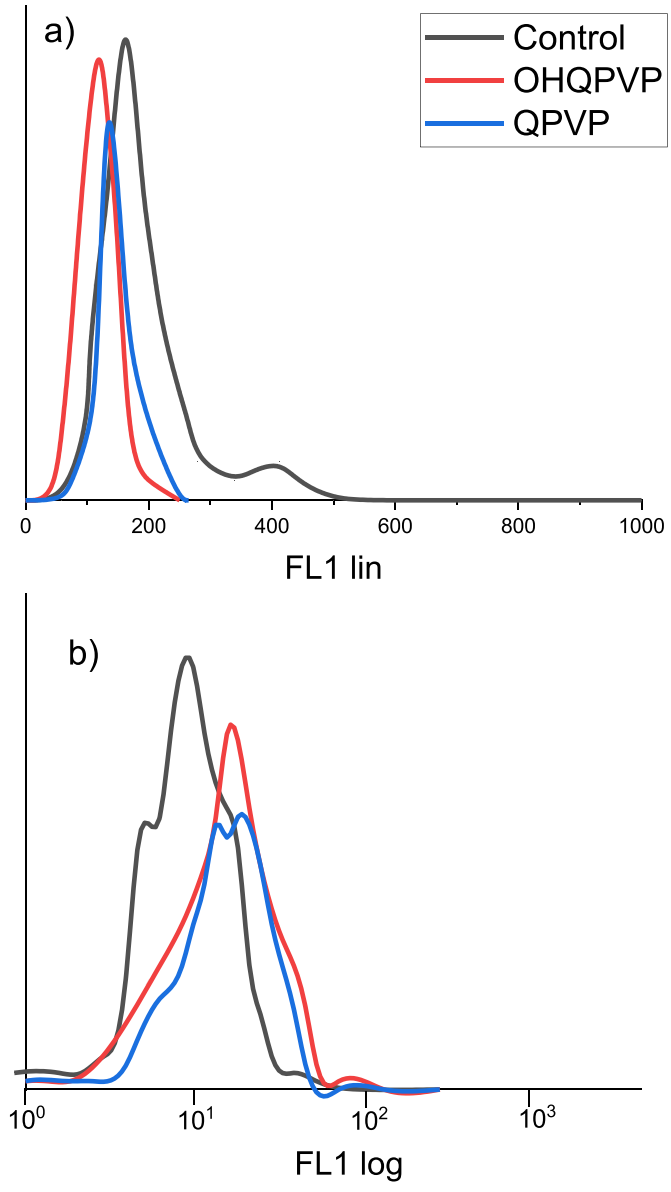

Fig. 3. Effects produced by OHQPVP and QPVP on the fluoresence of a cell population loaded with the probes DIBAC4(3) (a) and H_2DCFA (b). The concentrations used were 50 mg/L for the polycations and 2.6 × 10^6 cells/mL for *M. aeruginosa*.

release of the anion indicator (DIBAC4(3)) from the cell into the medium, the fluorescence decreased. Thus, the shift of the fluorescence peaks to lower values of the cyanobacterial suspensions treated with the polymers were due to the lower amount of DIBAC4(3) loading (Fig. 3a). Polymer internalization into cyanobacterial cells has been reported for PAMAM dendrimers, which was accompanied by a depolarization effect on the cytoplasmic membrane potential (Tamayo-Belda et al., 2019), but the opposite results obtained with QPVP and OHQPVP point to an effect on the ionic membrane permeability and/or ionic transmembrane gradient and not to their internalization.

The presence of both polymers also caused intracellular oxidative stress enhancing the production of ROS as reflected in the upward shift of the fluorescence peaks due to the probe H_2DCFA (Fig. 3b). ROS are formed along the electron transport chain (ETC) in respiratory and photosynthesis processes and its excess can affect cell viability (Rzymski et al., 2020). The cytoplasmic membrane potential is mainly determined by the ETC and proton extrusion to the cell exterior during photosynthesis (Zhang et al., 2020). The interaction of the polymer molecules with the membranes affected their permeability, collapsing the H^+ gradient of the plasma membrane uncoupling of the ETC, overproduction of ROS and leading to cell death. The observed higher toxicity of the OHQPVP polymer, as compared to that of QPVP, may be explained by a greater perturbation of the cell membrane due to higher partitioning. This is linked to its H-bonding capacity between the hydroxyl moieties of the polymer with the H-bond acceptor groups located in the membrane, thus increasing the permeability of the bilayer; similar to the effect of intramolecular hydrogen bond formation that decreases the barrier for small molecule translocation resulting in increased permeability (Coimbra et al., 2021).

3.3. Removal of cyanobacteria by clay-polymer composites

In this section, the effect of different composites on the flocculation of a suspension of cyanobacteria was studied, showing that the best performance was with the CH_3-PGC composite and the rationale behind. The influence on this coagulflocculant of variables such as pH and T, and the state of the coagulated cyanobacteria were also analyzed.

The use of composites presented a general pattern independently of the composite used (grafted or adsorbed) and the polymer used, with the only exception of CH_3-PGC (Table 1). The percentages of cyanobacteria found in solution, as well as their status, were approximately 85% living cells remaining in solution after 1 h, which varied slightly after 24 h.

The percentages remaining in solution as dead cells were about 8%, with very low percentages retained on the surface of the composites. This pattern was also maintained after 24 h and, therefore, it can be inferred that cell viability was not affected by prolonging the contact time with the composites, unlike with the polymers *per se*.

The composite CH_3-PGC induced a large removal fraction of cyanobacteria cells, reaching values of 66 ± 6% after 1 h, that remained closely to that after 24 h, 74 ± 5%. A comparison of this value with others reported in the literature is difficult because of the heterogeneity in the concentrations of cyanobacteria and the experimental procedure used (Table S2). Most studies have focused on the use of biopolymers used as flocculants, which usually need an aid to increase their effectiveness, such as the presence of Ca^{2+} ions, to increase bridging between coagulated particles (Furusawa and Iwamoto, 2022). Other studies have focused on the derivatization of biopolymers (You et al., 2022) or synergic relation between between alga and bacteria (Sepehri et al., 2020). Coagulflocculation yields with the CH_3-PGC composite are generally lower than those of these studies (Table S2). However, the concentration of microorganisms was either lower or the highest effectiveness was observed at pHs that are not relevant in DWTPs (pH 4; Sun et al., 2015). The initial pH of the cyanobacteria solution hardly had influence on the effectiveness of CH_3-PGC as a coagulant (Table S3), because the polymer is fully quaternized. Only at high pH (9.3) the efficiency was slightly reduced. In contrast, temperature did exert a drastic effect on the concentration of flocculated cyanobacteria (Table S3). An increase in temperature increased the Brownian motion of the particles, hindering flocculation. Another parameter studied was the influence of the reaction time (rapid mixing). A decrease from 1h to 5 min produced identical flocculation results (Table S3).

The higher flocculant power of the CH_3-PGC composite relative to the others (Table 1) can be rationalized on the basis of the combined effect of the surface potential and the accessibility of the positively charged moieties to the outer cell membrane. Despite the fact that the cells are negatively charged, their retention by composites such as CH_3- and OH-MMT was minimal, even though these had similar surface potentials to the grafted complexes. In the adsorbed complexes, the polymer molecules are intercalated and are hardly in close contact with the cells, unlike those with grafted polymers. This fact suggests that in addition to the complexes having a positive surface potential, there must be some accessibility of the polymer molecules to the cells. The higher retention by the CH_3-PGC composite can thus be explained by the combination of its high surface potential reaching a critical value for cell adhesion together with the higher accessibility of the polymer when tethered to the cell surface in a brush conformation. The OH-PGC composite was not effective because at the pH of the cyanobacterial suspension (7.7), its surface potential decreased greatly, from +34 mV (determined at pH 4, Fig. 1c) to +21 mV. This was due to the presence of non-quaternized moieties in the polymer, which deprotonated with increasing pH, reducing the positive charge of the complex, and decreasing its affinity for the cell surfaces. As inferred in Table 1, the toxicity of the OH-PGC composite was negligible with respect to the polymer OHQPVP (Fig. 2). This was likely due to the greatly reduced concentration of positively charged monomers interacting with the cells when the polymer molecules are tethered in a brush conformation (only those on the external surface of the brushes). The concentration of these monomers did not reach the critical concentration for induced perturbation into the cellular membrane increasing its permeabilization.

Cationic polymers with little toxicity in solution, once formulated with a clay mineral, can develop cydal effects. At a fixed polymer concentration, the higher concentration of cationic monomers in small discrete entities, such as the clay particles relative to the equivalent concentration of polymer in solution, can reach lethal levels for microorganisms (Undabeytia et al., 2014). The status of the removed cells on the composite surface was determined for CH_3-PGC by three experimental procedures: (i) release of cyanotoxins; (ii) extraction of adsorbed

Table 1
Cyanobacteria distribution after incubation as a function of time. The initial concentration of *M. aeruginosa*, 3.71 × 10^6 cells/mL.

Incubation time: 1 h			
	Retained/Sorbed (%)	Solution, live (%)	Solution, dead (%)
Polymers			
QPVP	–	97.53 ± 1.79	2.47 ± 1.55
OHQPVP	–	65.55 ± 3.50	34.45 ± 2.64
Composites			
PGC	2.71 ± 2.02	86.61 ± 2.09	8.98 ± 0.07
CH_3-PGC	66.08 ± 5.84	30.97 ± 5.36	2.95 ± 0.48
OH-PGC	5.93 ± 3.27	85.83 ± 3.09	8.24 ± 0.18
CH_3-MMT	3.49 ± 2.58	86.77 ± 1.08	7.74 ± 0.51
OH-MMT	4.09 ± 3.05	85.28 ± 2.00	10.63 ± 1.05
Incubation time: 24 h			
	Retained/Sorbed (%)	Solution, live (%)	Solution, dead (%)
Polymers			
QPVP	–	20.06 ± 0.02	79.94 ± 2.8
OHQPVP	–	4.23 ± 0.16	95.77 ± 0.21
Composites			
PGC	1.84 ± 0.72	80.45 ± 0.88	19.39 ± 0.16
CH_3-PGC	73.87 ± 4.91	19.59 ± 3.26	6.54 ± 1.65
OH-PGC	3.23 ± 0.14	78.47 ± 1.50	19.84 ± 0.69
CH_3-MMT	1.08 ± 0.23	79.69 ± 0.11	21.39 ± 0.12
OH-MMT	1.02 ± 0.31	76.42 ± 0.18	22.55 ± 0.13

cells followed by determination of their status; and (iii) confocal microscopy. In case of cellular death, release of endotoxin is expected but the amount determined in solution did not show any increase (Table 2).

Extraction of the cells located on the surface of the composite followed by flow cytometry analysis showed that 85 ± 5% were alive. The difference observed if all cells were alive is small, 10–15%, which may be due to errors inherent to the experimental procedure. The CLSM results of the cyanobacteria after interaction with the composite showed a green and red fluorescence representing the composite and the chorophyll autofluorescence of the cyanobacterial cells, respectively (Fig. 4). The red fluorescence was intense and analogous to the stock culture (Fig. S3), indicating that *Microcystis* cells supported on the surface were intact and healthy.

3.4. Study of the flocculation mechanism

As the CH_3-PGC composite concentration increased, a parallel correlation was observed between the turbidity values and the residual amounts of live cells in the supernatant (Fig. 5). At a composite concentration equivalent to 10 mg/L, the concentration of cells was reduced by 30% and the turbidity by 50%. At this concentration, the zeta potential is reversed reaching a positive value that remains constant at higher composite concentrations, where some reduction in the values of turbidity and cells in the supernatant was still observed at a two-fold concentration of the composite. These values increased with higher composite concentrations. The higher flocculation yield obtained after charge reversal was achieved whereas the zeta potential was maintained indicating that a charge neutralization mechanism could be dismissed (Sun et al., 2015).

The dimensions of a clay platelet can be estimated as a rectangular base formed by the siloxane plane of 0.7 × 1.5 μm and height of 1–2 μm (Stefanescu et al., 2006). The permanent negative charge of the clay resides in the basal plane which has been modified by cationic polymer grafting reactions causing charge reversal. A *M. aeruginosa* cell can be estimated as a spherical particle of diameter between 4 and 6 μm. Geometrically it is feasible for a cell to interact with several composite particles. At lower composite concentrations, the polymer tethered to the clay surface interacted with the negatively charged cell surface, but did not neutralize the overall charge only that locally in close contact. Interactions of negatively charged patches of the cell with polymer brushes of other particles induced their flocculation (Bolto and Gregory, 2007). The charge of each composite particle is not neutralized when interacting with the cell as inferred from the positive values of the zeta potential, only that fraction in close contact with the cell. The addition of an excess of positive charge with increasing composite concentration increased the electrostatic repulsion between the composite particles with their subsequent restabilization, increasing the turbidity and with fewer flocculated cells.

In Fig. 5, the highest flocculation achieved was at an equivalent composite dose of 20 mg/L polymer, which is within the values reported in the literature (Table S2). The coagulated fraction was 92.4% and the optimum ratio between the amount of coagulated cyanobacteria and this composite was 7.2×10^7 cells/mg polymer.

Table 2
LR-microcystin concentrations of coaguflocculated suspensions of *M. aeruginosa* treated with clay-polymer composites. The cyanobacterial concentration was 3.71×10^6 cells/mL.

	MC-LR concentration (μg L^{-1})
Initial	3.72 ± 0.94
OH-MMT	4.93 ± 0.78
PGC	2.73 ± 0.20
OHPGC	2.92 ± 0.46
CH_3-MMT	4.32 ± 0.98
CH_3-PGC	4.71 ± 1.24

3.5. Cyanobacteria removal in surface waters

The use of composites in surface waters required a higher dose to achieve coagulation efficiencies similar to those observed previously (Fig. 6). An efficiency of 35% was obtained using a dose of 100 mg/L, whereas this percentage was obtained with 40 mg/L using a cyanobacterial concentration one order-of-magnitude higher in an axenic culture (Fig. 5). An optimal coagulant dosage should have been lower than a composite concentration equivalent to 20 mg/L of polymer, when using a lower cyanobacterial concentration, since less complexes are needed to neutralize the cell charge. Thus resuspension of the particles by repulsive forces between the positively charged composite particles is avoided. On the contrary, the coagulation efficiency continues to increase with the composite concentration.

The higher coagulant demand required in surface waters was due to the nature of NOM. In addition to allelogenous organic matter, the composition of which differs according to the species present (Henderson et al., 2008), there are also humic and fulvic components. An indicator of NOM quality is the measurement of SUV_{254}. These values were low, the value determined in surface water was about two-fold higher (2.00 ± 0.03 L/(m^{-1} mg C^{-1})) than that determined in axenic cultures (1.14 ± 0.01 L/(m^{-1} mg C^{-1})), related to a higher content of conjugated double bonds and aromatic structures (Pivokonsky et al., 2015). The lower coagulation efficiency would be due to the higher hydrophobicity of the NOM in surface waters (Fu et al., 2019) when the main flocculation mechanism involves electrostatic interactions. The coagulation efficiency is also dependent on the cellular morphology (González-Torres et al., 2019). Lama et al. (2016) reported that the minium flocculant dosage for inducing flocculation of nine species of unicellular microalgae and one cyanobacterium with the polymer chitosan had a coefficient of variation of 69%. Species other than *M. aeruginosa* were detected in minor amounts in this surface water (Fuente et al., 2019), which may hamper the flocculation process.

4. Conclusions

Clay-based composites can be designed using polymers that coagulate cyanobacterial suspensions, preventing lysis and endotoxin release. Despite the toxic effect of the polymers used, the designed composites showed null toxicity. The composites obtained by sorption showed the absence of the Tg at 124 and 180 °C of OHQPVP and QPVP polymers, respectively. X-ray diffraction peaks of the composites at 1.55 nm indicated a train conformation of the polymer molecules on the clay surface, avoiding easily detachable molecules on the external surface of the clay Infrared spectroscopy showed that not all of the pyridinyl nitrogen in OHQPVP composites was quaternized. The CH_3-PGC composite was the only one that performed as a good coaguflocculant, reaching removal values of 92 ± 2% of coaguflocculated cells from a *M. aeruginosa* suspension of 1.56×10^6 cells/mL, using an amount equivalent to 20 mg/L of polymer. The optimization of a clay-polymer composite required a high surface potential and a very close interaction of the cationic moieties of the polymer with the negatively charged cell surface, but at concentrations below those necessary for the development of toxicity, as occurs in a brush conformation with grafted polymers. This was only achieved with the CH_3-PGC composite, due to charge reduction of the OH-PGC from +34 to +21 mV associated to deprotonation of N at the pH of the cyanobacterial suspensions. A patch mechanism was dominant in the flocculation of cyanobacterial cells by the CH_3-PGC composite. In surface waters, a key factor is the presence of NOM which increased the required coagulant dose of the composite relative to that determined in axenic cyanobacterial cultures. This study establishes the basis for the development of polymer-clay mineral composites that act as good coagulants for cyanobacterial suspensions.

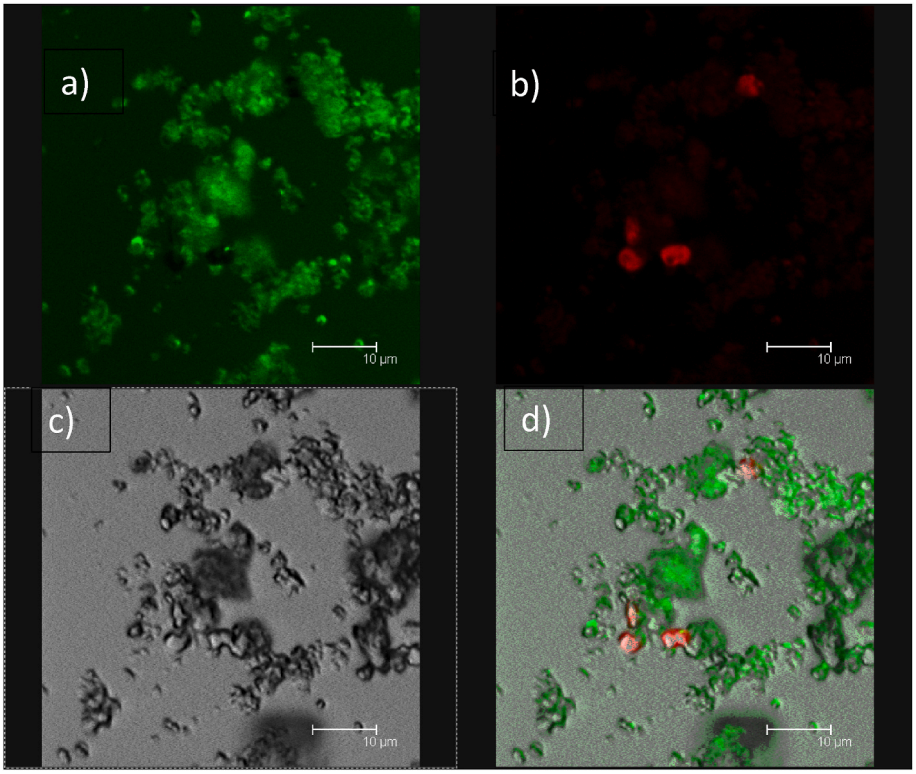

Fig. 4. CLSM images of the cells interacting with the CH_3-PGC composite: (a) supporting composite (a) (green fluorescence); (b) cells (red autofluorescence); (c) optical micrograph; and (d) composed image. (For interpretation of the references to colour in this figure legend, the reader is referred to the Web version of this article.)

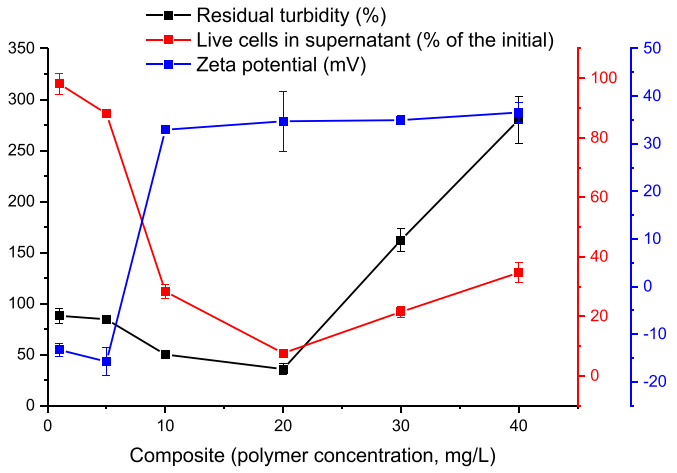

Fig. 5. Live cells, residual turbidity and zeta potential of a *M. aeruginosa* suspension as a function of the composite dose expressed as the amount of equivalent polymer. The concentration of *M. aeruginosa* was 1.56×10^6 cells/mL.

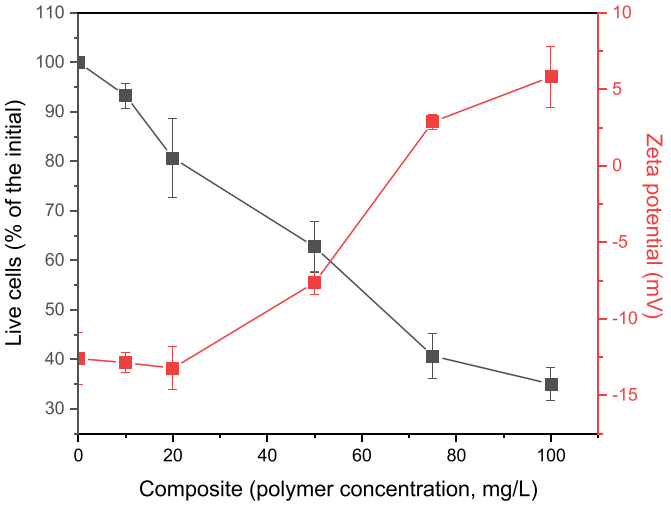

Fig. 6. Live cells and zeta potential of a cyanobacteria bloomed surface water containing 1.35×10^6 cells/mL treated with increasing CH_3-PGC concentrations.

CRediT authorship contribution statement

Ido Gardi: Conceptualization, Investigation. **Yael-Golda Mishael:** Conceptualization. **Marika Lindahl:** Investigation, Visualization. **Alicia M. Muro-Pastor:** Investigation. **Tomás Undabeytia:** Conceptualization, Investigation, writing.

Declaration of competing interest

The authors declare that they have no known competing financial interests or personal relationships that could have appeared to influence the work reported in this paper.

Data availability

Data will be made available on request.

Acknowledgments

This work has received financial support from the Spanish Ministry

of Science and Innovation (project CTM2016-77168-R). The authors also acknowledge the Services of the University of Seville (CITIUS) of Biology for flow cytometer analysis, and of Microanalysis and Functional Characterisation for determination of zeta potentials, loading of the polymers and MC-LR analysis. They also acknowledge the Microscopy Service of the CIC Isla de la Cartuja.

Appendix A. Supplementary data

Supplementary data to this article can be found online at https://doi.org/10.1016/j.jclepro.2023.136356.

References

Backer, L., Baptiste, D.M., Le Prell, R., Bolton, B., 2015. Cyanobacteria and algae blooms: review of health and environmental data from the harmful algal bloom-related illness surveillance system (HABISS) 2007–2011. Toxins 7, 1048–1064.

Bolto, G., Gregory, J., 2007. Organic polyelectrolytes in water treatment. Water Res. 41, 2301–2324.

Coimbra, J.T.S., Feghali, R., Ribeiro, R.P., Ramos, M.J., Fernandes, P.A., 2021. The importance of intramolecular hydrogen bonds on the translocation of the small drug piracetam through a lipid bilayer. RSC Adv. 11, 899–908.

Dang, A., Hui, C.-M., Ferebee, R., Kubiak, J., Li, T., Matyjaszewski, K., Bockstaller, M.R., 2013. Thermal properties of particle brush materials: effect of polymer graft architecture on the glass transition temperature in polymer-grafted colloidal systems. Macromol. Symp. 331–332, 9–16.

Du, Y., Ye, J., Wu, L., Yang, C., Wang, L., Hu, X., 2017. Physiological effects and toxin release in *Microcystis aeruginosa* and *Microcystis viridis* exposed to herbicide fenoxaprop-p-ethyl. Environ. Sci. Pollut. Res. 24, 7752–7763.

Du, X., Liu, H., Wang, Y., Ma, Y., Wang, R., Chen, X., Losiewicz, M.D., Guo, H., Zhang, H., 2019. The diversity of cyanobacterial toxins on structural characterization, distribution and identification: a systematic review. Toxins 11, 530. https://doi.org/10.3390/toxins11090530.

Fu, H.Y., Liu, K., Alvarez, P.J.J., Yin, D.Q., Qu, X.L., Zhu, D.Q., 2019. Quantifying hydrophobicity of natural organic matter using partition coefficients in aqueous two-phase systems. Chemosphere 218, 922–929.

Fuente, A. de la, Muro-Pastor, A., Merchán, F., Madrid Díaz, F., Pérez-Martínez, J.I., Undabeytia, T., 2019. Electrocoagulation/flocculation of cyanobacteria from surface waters. J. Clean. Prod. 238, e117964.

Furusawa, G., Iwamoto, K., 2022. Removal of *Microcystis aeruginosa* cells using the dead cells of a marine filamentous bacterium, *Aureispira* sp. CCB-QB1. PeerJ, e12867.

Ganigar, R., Rytwo, G., Gonen, Y., Radian, A., Mishael, Y.G., 2010. Polymer–clay nanocomposites for the removal of trichlorophenol and trinitrophenol from water. Appl. Clay Sci. 49, 311–316.

Gardi, I., Mishael, Y.G., 2018. Designing a regenerable stimuli-responsive grafted polymer-clay sorbent for filtration of water pollutants. Sci. Technol. Adv. Mater. 19, e589.

Gerchman, Y., Vasker, B., Tavasi, M., Mishael, Y., Kinel-Tahan, Y., Yehoshua, Y., 2017. Effective harvesting of microalgae: comparison of different polymeric flocculants. Bioresour. Technol. 228, 141–146.

Ghernaout, B., Ghernaout, D., Saiba, A., 2010. Algae and cyanotoxins removal by coagulation/flocculation: a review. Desalination Water Treat. 20, 133–143.

Ghernaout, D., Ghernaout, B., 2012. Sweep flocculation as a second form of charge neutralization-A review. Desalination Water Treat. 44, 15–28.

Gomes, A., Fernandes, E., Lima, J.L.F.C., 2005. Fluorescence probes used for detection of reactive oxygen species. J. Biochem. Biophys. Methods 65, 45–80.

González-Torres, A., Pivokonsky, M., Henderson, R.K., 2019. The impact of cell morphology and algal organic matter on algal floc properties. Water Res. 163, e114887.

He, X., Liu, Y.-L., Conklin, A., Wrestrick, J., Weavers, L.K., Dionysiou, D.D., Lenhart, J.J., Mouser, P.J., Szlag, D., Walker, H.W., 2016. Toxic cyanobacteria and drinking water: impacts, detection and treatment. Harmful Algae 54, 174–193.

Henderson, R., Parsons, S.A., Jefferson, B., 2008. The impact of algal properties and pre-oxidation on solid-liquid separation of algae. Water Res. 42, 1827–1845.

Huh, J.-H., Ahn, J.-W., 2017. A perspective of chemical treatment for cyanobacteria control toward sustainable freshwater development. Environ. Eng. Res. 22, 1–11.

Huisman, J., Codd, G.A., Paerl, H.W., Ibelings, B.W., Verspagen, J.M.H., Visser, P.M., 2018. Cyanobacterial blooms. Nat. Rev. Microbiol. 16 https://doi.org/10.1038/s41579-018-0040-1.

Kohay, H., Izbitski, A., Mishael, Y.G., 2015. Developing polycation-clay sorbents for efficient filtration of diclofenac: effect of dissolved organic matter and comparison to activated carbón. Environ. Sci. Technol. 49, 9280–9288.

Kohay, H., Bilkis, I.I., Mishael, Y.G., 2019. Effect of polycation charge density on polymer conformation at the clay surface and consequently on pharmaceutical binding. J. Colloid Interface Sci. 552, 517–527.

König, R.B., Sales, R., Roselet, F., Abreu, P.C., 2014. Harvesting of the marine microalga Conticribra weissflogii (Bacillariophyceae) by cationic polymeric flocculants. Biomass Bioenergy 68, 1–6.

Lal, K., Garg, A., 2019. Effectiveness of synthesized aluminum and iron based inorganic polymer coagulants for pulping wastewater treatment. J. Environ. Chem. Eng. 7, e103204.

Lama, S., Muylaert, K., Karki, T.B., 2016. Flocculation properties of several microalgae and a cyanobacterium species during ferric chloride, chitosan and alkaline flocculation. Bioresour. Technol. 220, 464–470.

Letelier-Gordo, C.O., Holdt, S.L., Francisci, D.de, Karakashev, D.B., Angelidaki, I., 2014. Effective harvesting of the microalgae Chlorella protothecoides via bioflocculation with cationic starch. Bioresour. Technol. 167, 214–218.

Levy, L., Izbitski, A., Mishael, Y.G., 2019. Enhanced gemfibrozil removal from treated wastewater by designed "loopy" clay-polycation sorbents: effect of diclofenac and effluent organic matter. Appl. Clay Sci. 182, e105278.

Pivokonsky, M., Naceradska, J., Kopecka, I., Baresova, M., Jefferson, B., Li, X., Henderson, K., 2015. The impact of algogenic organic matter on water treatment plant operation and water quality: a review. Crit. Rev. Environ. Sci. Technol. 46, 291–335.

Rzymski, P., Klimaszyk, P., Jurczak, T., Poniedziatek, B., 2020. Oxidative stress, programmed cell death and microcystin release in Microcystis aeruginosa in response to Daphnia grazers. Front. Microbiol. 11, e1201.

Sepehri, A., Sarrafzadeh, M.-H., Ayateffazeli, M., 2020. Interaction between Chlorella vulgaris and nitrifying-enriched activated sludge in the treatment of wastewater with low C/N ratio. J. Clean. Prod. 247, e119164.

Sorlini, S., Collivignarelli, M.C., Abbà, A., 2018. Control measures for cyanobacteria and cyanotoxins in drinking water. Environ. Eng. Manag. J. 17, 2455–2463.

Stefanescu, E.A., Dundigalla, A., Ferreiro, V., Loizou, E., Porcar, L., Negulescu, I., Garnoa, J., Schmidt, G., 2006. Supramolecular structures in nanocomposite multilayered films. Phys. Chem. Chem. Phys. 8, 1739–1746.

Sun, P., Bai, N., Yang, S., Wan, L., Zhang, Q., Zhao, Y., 2015. Revealing the characteristics of a novel bioflocculant and its flocculation performance in Microcystis aeruginosa removal. Sci. Rep. 5, e17465.

Tamayo-Belda, M., González-Pleiter, M., Pulido-Reyes, G., Martín-Betancor, K., Leganés, F., Rosal, R., Fernández-Piñas, F., 2019. Mechanism of the toxic action of cationic G5 and G7 PAMAM dendrimers in the cyanobacterium Anabaena sp. PCC120. Environ. Sci. Nano 6, 863–878.

Theng, B.K.G., 2012. Formation and properties of clay-polymer complexes. In: Developments in Clay Science. Elsevier, Amsterdam.

Tran, D.-T., Le, B.-H., Lee, D.-J., Chen, C.-L., Wang, H.-Y., Chang, J.-S., 2013. Microalgae harvesting and subsequent biodiesel conversion. Bioresour. Technol. 140, 179–186.

Undabeytia, T., Posada, R., Nir, S., Galindo, I., Laiz, L., Saiz-Jiménez, C., Morillo, E., 2014. Removal of waterborne microorganisms by filtration using clay–polymer complexes. J. Hazard Mater. 279, 290–296.

Westrick, J.A., Szlag, D.C., Southwell, B.J., Sinclair, J., 2010. A review of cyanobacteria and cyanotoxins removal/inactivation in drinking water treatment. Anal. Bioanal. Chem. 397, 1705–1714.

Wolff, C., Fuks, B., Chatelain, P., 2003. Comparative study of membrane potential-sensitive fluorescent probes and their use in ion cannel screening assays. J. Biomol. Screen 8, 533–543.

You, Y., Yang, L., Sun, X., Chen, H., Wang, H., Wang, N., Li, S., 2022. Synthesized cationic starch grafted tannin as a novel flocculant for efficient microalgae harvesting. J. Clean. Prod. 344, e131042.

Zhang, M., Steinman, A.D., Xue, Q., Zhao, Y., Xu, Y., Xie, L., 2020. Effects of erythromycin and sulfamethoxazole on Microcystis aeruginosa: cytotoxic endpoints, production and release of microcystin-LR. J. Hazard Mater. 399, e123021.

Zhuo, B., Zhang, S., Niu, C., Zhou, H., Sun, S., Wang, X., 2017. Grafting density dominant glass transition of dry polystyrene brushes. Soft Matter 13, 2426–2436.